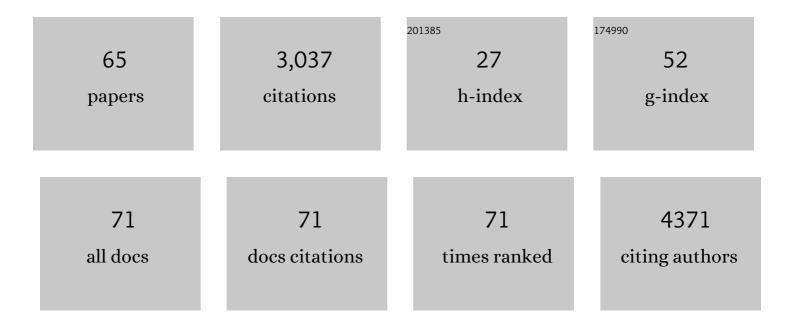
Matthias Wilmanns

List of Publications by Year in descending order

Source: https://exaly.com/author-pdf/4618642/publications.pdf Version: 2024-02-01



#	Article	IF	CITATIONS
1	Synergy of protease-binding sites within the ecotin homodimer is crucial for inhibition of MASP enzymes and for blocking lectin pathway activation. Journal of Biological Chemistry, 2022, 298, 101985.	1.6	4
2	Versatile allosteric properties in Pex5â€like tetratricopeptide repeat proteins to induce diverse downstream function. Traffic, 2021, 22, 140-152.	1.3	4
3	The XBI BioLab for life science experiments at the European XFEL. Journal of Applied Crystallography, 2021, 54, 7-21.	1.9	23
4	Molecular basis for the allosteric activation mechanism of the heterodimeric imidazole glycerol phosphate synthase complex. Nature Communications, 2021, 12, 2748.	5.8	22
5	Structure of the mycobacterial ESX-5 type VII secretion system pore complex. Science Advances, 2021, 7, .	4.7	45
6	Conserved and specialized functions of Type VII secretion systems in non-tuberculous mycobacteria. Microbiology (United Kingdom), 2021, 167, .	0.7	14
7	Across scales: novel insights into kidney health and disease by structural biology. Kidney International, 2021, 100, 281-288.	2.6	0
8	TBX2 controls a proproliferative gene expression program in melanoma. Genes and Development, 2021, 35, 1657-1677.	2.7	7
9	Mechanism of conditional partner selectivity in MITF/TFE family transcription factors with a conserved coiled coil stammer motif. Nucleic Acids Research, 2020, 48, 934-948.	6.5	17
10	The ATPases of the mycobacterial type VII secretion system: Structural and mechanistic insights into secretion. Progress in Biophysics and Molecular Biology, 2020, 152, 25-34.	1.4	11
11	The crystal structure of mycobacterial epoxide hydrolase A. Scientific Reports, 2020, 10, 16539.	1.6	4
12	Structure-Based Identification and Functional Characterization of a Lipocalin in the Malaria Parasite Plasmodium falciparum. Cell Reports, 2020, 31, 107817.	2.9	23
13	The <scp>pMy</scp> vector series: A versatile cloning platform for the recombinant production of mycobacterial proteins in <i>Mycobacterium smegmatis</i> . Protein Science, 2020, 29, 2528-2537.	3.1	9
14	Multiscale computation delivers organophosphorus reactivity and stereoselectivity to immunoglobulin scavengers. Proceedings of the National Academy of Sciences of the United States of America, 2020, 117, 22841-22848.	3.3	13
15	Uncovering targeting priority to yeast peroxisomes using an in-cell competition assay. Proceedings of the National Academy of Sciences of the United States of America, 2020, 117, 21432-21440.	3.3	17
16	Tuning Transcription Factor Availability through Acetylation-Mediated Genomic Redistribution. Molecular Cell, 2020, 79, 472-487.e10.	4.5	38
17	1H, 13C, and 15N backbone assignments of the C-terminal region of the human retinoic acid-induced protein 2. Biomolecular NMR Assignments, 2020, 14, 271-275.	0.4	1
18	A kinase bioscavenger provides antibiotic resistance by extremely tight substrate binding. Science Advances, 2020, 6. eaaz9861.	4.7	17

MATTHIAS WILMANNS

#	Article	IF	CITATIONS
19	Structural basis of p62/SQSTM1 helical filaments and their role in cellular cargo uptake. Nature Communications, 2020, 11, 440.	5.8	71
20	Gain-of-Function Variant p.Pro2555Arg of von Willebrand Factor Increases Aggregate Size through Altering Stem Dynamics. Thrombosis and Haemostasis, 2020, , .	1.8	3
21	Subcellular localization and stability of <scp>MITF</scp> are modulated by the <scp>bHLH</scp> â€Zip domain. Pigment Cell and Melanoma Research, 2019, 32, 41-54.	1.5	23
22	MITF has a central role in regulating starvation-induced autophagy in melanoma. Scientific Reports, 2019, 9, 1055.	1.6	66
23	An NAD+ Phosphorylase Toxin Triggers Mycobacterium tuberculosis Cell Death. Molecular Cell, 2019, 73, 1282-1291.e8.	4.5	58
24	Structural diversity in the atomic resolution 3D fingerprint of the titin M-band segment. PLoS ONE, 2019, 14, e0226693.	1.1	1
25	Structural Variability of EspG Chaperones from Mycobacterial ESX-1, ESX-3, and ESX-5 Type VII Secretion Systems. Journal of Molecular Biology, 2019, 431, 289-307.	2.0	21
26	The von Willebrand factor Tyr2561 allele is a gain-of-function variant and a risk factor for early myocardial infarction. Blood, 2019, 133, 356-365.	0.6	24
27	Structure and dynamics of the platelet integrin-binding C4 domain of von Willebrand factor. Blood, 2019, 133, 366-376.	0.6	22
28	The Von Willebrand Factor Tyr2561 Allele Is a Gain-of-Function Variant and a Potential Risk Factor for Early Myocardial Infarction. Blood, 2018, 132, 2459-2459.	0.6	1
29	Structure of the mycobacterial ESX-5 type VII secretion system membrane complex by single-particle analysis. Nature Microbiology, 2017, 2, 17047.	5.9	102
30	Intermolecular base stacking mediates RNA-RNA interaction in a crystal structure of the RNA chaperone Hfq. Scientific Reports, 2017, 7, 9903.	1.6	14
31	Model-based local density sharpening of cryo-EM maps. ELife, 2017, 6, .	2.8	200
32	Higherâ€order assemblies of oligomeric cargo receptor complexes form the membrane scaffold of the Cvt vesicle. EMBO Reports, 2016, 17, 1044-1060.	2.0	26
33	Towards the molecular mechanism of the integration of peroxisomal membrane proteins. Biochimica Et Biophysica Acta - Molecular Cell Research, 2016, 1863, 863-869.	1.9	18
34	A standardized production pipeline for high profile targets from Mycobacterium tuberculosis. Proteomics - Clinical Applications, 2016, 10, 1049-1057.	0.8	5
35	Robotic QM/MM-driven maturation of antibody combining sites. Science Advances, 2016, 2, e1501695.	4.7	15
36	Death-Associated Protein Kinase Activity Is Regulated by Coupled Calcium/Calmodulin Binding to Two Distinct Sites. Structure, 2016, 24, 851-861.	1.6	21

MATTHIAS WILMANNS

#	Article	IF	CITATIONS
37	Structural biology of the import pathways of peroxisomal matrix proteins. Biochimica Et Biophysica Acta - Molecular Cell Research, 2016, 1863, 804-813.	1.9	45
38	Suppression of Early Hematogenous Dissemination of Human Breast Cancer Cells to Bone Marrow by Retinoic Acid–Induced 2. Cancer Discovery, 2015, 5, 506-519.	7.7	45
39	Characterization of the Mycobacterial Acyl-CoA Carboxylase Holo Complexes Reveals Their Functional Expansion into Amino Acid Catabolism. PLoS Pathogens, 2015, 11, e1004623.	2.1	19
40	Structural Insights into Cargo Recognition by the Yeast PTS1 Receptor. Journal of Biological Chemistry, 2015, 290, 26610-26626.	1.6	27
41	Ligandâ€Induced Compaction of the <scp>PEX5</scp> Receptorâ€Binding Cavity Impacts Protein Import Efficiency into Peroxisomes. Traffic, 2015, 16, 85-98.	1.3	37
42	Induction of insulin-like growth factor 1 splice forms by subfragments of myofibrillar proteins. Molecular and Cellular Endocrinology, 2015, 399, 69-77.	1.6	9
43	Refined Requirements for Protein Regions Important for Activity of the TALE AvrBs3. PLoS ONE, 2015, 10, e0120214.	1.1	29
44	Role of κ→λ light-chain constant-domain switch in the structure and functionality of A17 reactibody. Acta Crystallographica Section D: Biological Crystallography, 2014, 70, 708-719.	2.5	22
45	Crystal structure of the VapBC-15 complex from Mycobacterium tuberculosis reveals a two-metal ion dependent PIN-domain ribonuclease and a variable mode of toxin–antitoxin assembly. Journal of Structural Biology, 2014, 188, 249-258.	1.3	47
46	Structure of the <scp><i>M</i></scp> <i>ycobacterium tuberculosis</i> type <scp>VII</scp> secretion system chaperone <scp>EspG</scp> ₅ in complex with <scp>PE</scp> 25– <scp>PPE</scp> 41 dimer. Molecular Microbiology, 2014, 94, 367-382.	1.2	83
47	WXG100 Protein Superfamily Consists of Three Subfamilies and Exhibits an α-Helical C-Terminal Conserved Residue Pattern. PLoS ONE, 2014, 9, e89313.	1.1	92
48	Crystal structure of the S187F variant of human liver alanine: Aminotransferase associated with primary hyperoxaluria type I and its functional implications. Proteins: Structure, Function and Bioinformatics, 2013, 81, 1457-1465.	1.5	24
49	MITF mutations associated with pigment deficiency syndromes and melanoma have different effects on protein function. Human Molecular Genetics, 2013, 22, 4357-4367.	1.4	50
50	Molecular Requirements for Peroxisomal Targeting of Alanine-Glyoxylate Aminotransferase as an Essential Determinant in Primary Hyperoxaluria Type 1. PLoS Biology, 2012, 10, e1001309.	2.6	64
51	Restricted leucine zipper dimerization and specificity of DNA recognition of the melanocyte master regulator MITF. Genes and Development, 2012, 26, 2647-2658.	2.7	103
52	Catalysis Uncoupling in a Glutamine Amidotransferase Bienzyme by Unblocking the Glutaminase Active Site. Chemistry and Biology, 2012, 19, 1589-1599.	6.2	40
53	Improved mycobacterial protein production using a Mycobacterium smegmatis groEL1î"Cexpression strain. BMC Biotechnology, 2011, 11, 27.	1.7	51
54	Proteomeâ€wide identification of mycobacterial pupylation targets. Molecular Systems Biology, 2010, 6, 386.	3.2	94

MATTHIAS WILMANNS

#	Article	IF	CITATIONS
55	Stoichiometric protein complex formation and overâ€expression using the prokaryotic native operon structure. FEBS Letters, 2010, 584, 669-674.	1.3	26
56	Solution Structure of Human Pex5·Pex14·PTS1 Protein Complexes Obtained by Small Angle X-ray Scattering. Journal of Biological Chemistry, 2009, 284, 25334-25342.	1.6	41
57	Structural basis for competitive interactions of Pex14 with the import receptors Pex5 and Pex19. EMBO Journal, 2009, 28, 745-754.	3.5	82
58	Structure-Based Approaches to Drug Discovery Against Tuberculosis. Current Protein and Peptide Science, 2007, 8, 365-375.	0.7	17
59	A previously unobserved conformation for the human Pex5p receptor suggests roles for intrinsic flexibility and rigid domain motions in ligand binding. BMC Structural Biology, 2007, 7, 24.	2.3	23
60	Recognition of a Functional Peroxisome Type 1 Target by the Dynamic Import Receptor Pex5p. Molecular Cell, 2006, 24, 653-663.	4.5	156
61	Topography for Independent Binding of α-Helical and PPII-Helical Ligands to a Peroxisomal SH3 Domain. Molecular Cell, 2002, 10, 1007-1017.	4.5	81
62	Structural Evidence for Ammonia Tunneling across the (βα)8 Barrel of the Imidazole Glycerol Phosphate Synthase Bienzyme Complex. Structure, 2002, 10, 185-193.	1.6	109
63	Efficient expression, purification and crystallisation of two hyperthermostable enzymes of histidine biosynthesis. FEBS Letters, 1999, 454, 1-6.	1.3	35
64	Structural basis for activation of the titin kinase domain during myofibrillogenesis. Nature, 1998, 395, 863-869.	13.7	333
65	High-resolution crystal structures of tyrosine kinase SH3 domains complexed with proline-rich peptides. Nature Structural Biology, 1994, 1, 546-551.	9.7	284